

Comparison of ZnO nanostructures grown using pulsed laser deposition, metal organic chemical vapor deposition, and physical vapor transport

V. E. Sandana^{a)}

Nanovation, 103B Rue de Versailles, 91400 Orsay, France; Center for Quantum Devices, Northwestern University, Evanston, Illinois 60208; and Department of Irradiated Solids, Ecole Polytechnique, 91128 Palaiseau, France

D. J. Rogers and F. Hosseini Teherani

Nanovation, 103B Rue de Versailles, 91400 Orsay, France

R. McClintock, C. Bayram, and M. Razeghi

Center for Quantum Devices, Northwestern University, Evanston, Illinois 60208

H.-J. Drouhin and M. C. Clochard

Department of Irradiated Solids, Ecole Polytechnique, 91128 Palaiseau, France

V. Sallet

GEMAC, 45 avenue des Etats-Unis, 78035 Versailles, France

G. Garry

Thales Research & Technology, Route Départementale 128, F-91767 Palaiseau, France

F. Falyouni

GEMAC, 45 avenue des Etats-Unis, 78035 Versailles, France

(Received 8 December 2008; accepted 27 April 2009; published 28 May 2009)

This article compares the forms and properties of ZnO nanostructures grown on Si(111) and *c*-plane sapphire (*c*-Al₂O₃) substrates using three different growth processes: metal organic chemical vapor deposition (MOCVD), pulsed laser deposition (PLD), and physical vapor transport (PVT). A very wide range of ZnO nanostructures was observed, including nanorods, nanoneedles, nanocombs, and some novel structures resembling “bevelled” nanowires. PVT gave the widest family of nanostructures. PLD gave dense regular arrays of nanorods with a preferred orientation perpendicular to the substrate plane on both Si and *c*-Al₂O₃ substrates, without the use of a catalyst. X-ray diffraction (XRD) studies confirmed that nanostructures grown by PLD were better crystallized and more highly oriented than those grown by PVT and MOCVD. Samples grown on Si showed relatively poor XRD response but lower wavelength emission and narrower linewidths in PL studies. © 2009 American Vacuum Society. [DOI: 10.1116/1.3137990]

I. INTRODUCTION

ZnO is a remarkable multifunctional material with a distinctive set of properties, including a direct bandgap of ~3.37 eV, high transparency over the visible spectrum, a very wide range of possible conductivities, and a strong piezoelectric response. Thus ZnO has many established and emerging applications including varistors, light emitting diodes¹ (LEDs) and surface acoustic wave devices.² Nanostructuring of ZnO³ further extends the range of potential applications by augmenting the basic property set with phenomena unique to the quantum world.⁴ Indeed, nanostructured ZnO has become a huge research topic with more publications in 2008 than even carbon nanotubes.⁵ There are many reasons driving this interest, including the unique property set of ZnO,⁶ the ease of fabrication of ZnO nanostructures with a wide range of techniques,⁷ the wide range of emerging and potential applications,⁸ the biocompatibility of ZnO,⁹ and the enormous family of nanostructures exhib-

ited by ZnO (probably the largest of any nanomaterial^{6,10}). Although ZnO has been grown with a vast range of different techniques, direct comparison of the properties of nanostructures grown with different methods is lacking in *the literature*. This article compares the forms, crystallographic properties, and optical properties of ZnO nanostructures prepared using three common growth processes: metal organic chemical vapor deposition (MOCVD), pulsed laser deposition (PLD), and physical vapor transport (PVT). Three different techniques were employed in order to facilitate exploration of the relative merits of each approach.

II. EXPERIMENT

Both Si (111) and *c*-plane sapphire (*c*-Al₂O₃) were used as substrates for the three growth processes.

A. MOCVD

ZnO was deposited by MOCVD [Fig. 1(a)] in a water-cooled vertical quartz reactor with an inner diameter of 40 mm in the growth zone. The Zn source was dimethyl zinc

^{a)}Electronic mail: sandana@nanovation.com

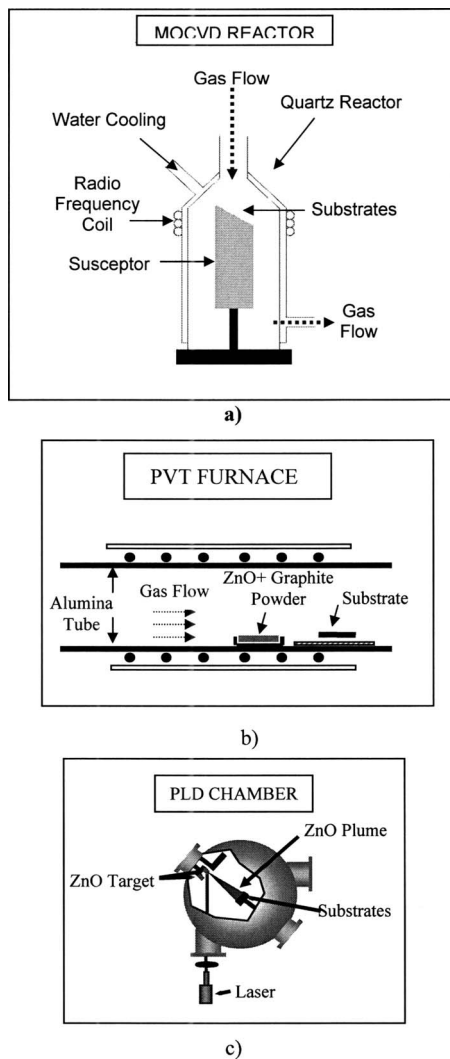


FIG. 1. Growth process schematics of (a) MOCVD, (b) PVT, and (c) PLD.

triethylamine (DZT) $[(\text{CH}_3)_2\text{Zn}-\text{N}(\text{CH}_2\text{CH}_3)_3]$ and the carrier gas was N_2 . The flow rate was 500 SCCM (SCCM denotes cubic centimeter per minute at STP) for the carrier gas and the DZT combined. N_2O gas was used as the O source and its flow rate was also 500 SCCM. The substrate was placed in the middle of the reactor on a graphite susceptor, which was inclined at 45° to the vertical. The susceptor was heated to 800°C during film growth using a radio frequency (rf) coil.

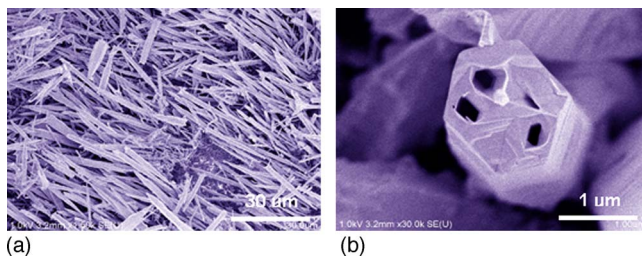


FIG. 2. (Color online) SEM images of ZnO on $c\text{-Al}_2\text{O}_3$ grown by MOCVD.

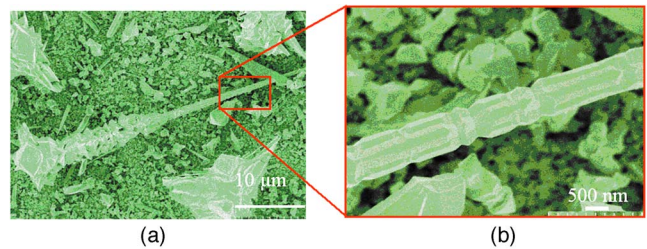


FIG. 3. (Color online) SEM images of ZnO grown on Si (111) by MOCVD.

B. PVT

ZnO was deposited by carbothermal evaporation in a tubular furnace with an inner diameter of 30 mm [Fig. 1(b)]. A 2 g (1:1 mass ratio) mix of ZnO and graphite powders was used for the growth and covered a 1 cm^2 surface. N_2 was used as the carrier gas at 80 SCCM gas flow rate. Both outlets of the furnace were kept open to ambient air. A ceramic holder with the powder was inserted into the quartz tube when the furnace temperature stabilized at 1100°C . The $c\text{-Al}_2\text{O}_3$ and Si (111) substrates were placed with a distance of 5 cm from the end of the powder boat to the beginning of the substrate. The reaction time was 30 min.

C. PLD

ZnO nanostructures were grown from a 99.99% pure ZnO target by PLD [Fig. 1(c)] using a KrF excimer laser (248 nm) as described elsewhere.^{11,12}

III. CHARACTERIZATIONS

The sample morphology was studied using a Hitachi S4800 field emission-scanning electron microscope (SEM). The crystal quality of the nanostructures was investigated using x-ray diffraction (XRD) performed in a Panalytical MRD Pro system using $\text{Cu K}\alpha$ radiation. The x-ray optics and spot size were kept the same for all samples. Optical properties were studied via room temperature photoluminescence (PL) with a continuous-wave frequency-doubled argon ion laser (244 nm, power of 30 mW).

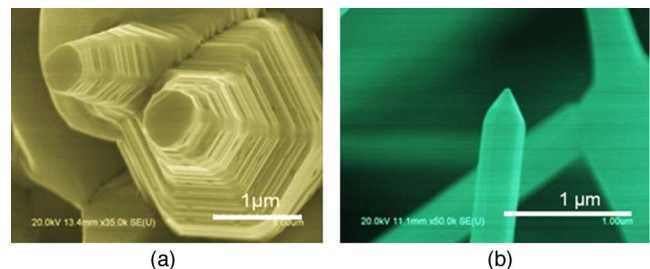


FIG. 4. (Color online) SEM images of ZnO nanostructures on $c\text{-Al}_2\text{O}_3$ grown by PVT.

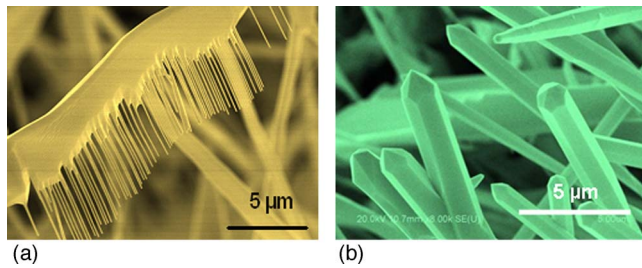


FIG. 5. (Color online) SEM images of ZnO nanostructures on Si(111) grown by PVT.

IV. RESULTS

A. SEM investigations

1. SEM images for MOCVD growth of ZnO

SEM images for MOCVD growth of ZnO on $c\text{-Al}_2\text{O}_3$. Figure 2(a) is a SEM image for a MOCVD growth on $c\text{-Al}_2\text{O}_3$. The image shows a forest of microcolumns/wires of rather uniform diameter and length (typically 1.5 and 30 μm , respectively). The majority of the columns have a preferred orientation perpendicular to the substrate plane. The higher magnification image shown in Fig. 2(b) reveals that some of these microstructures are partially hollowed, such that the best description of their form might be hexagonally faceted nanotubes. The origin of this hollowing is still under consideration.

SEM images for MOCVD growth of ZnO on Si (111). For growth on Si (111), a wide range of microstructures of varying form and size was obtained. For one particular region [expanded in Fig. 3(b)], an unusual microrod structure with 12 facets and a structure which resembles bevelling of a table leg were observed. The presence of this atypical microstructure could be related to an effect of the Si substrate, since microstructures on $c\text{-sapphire}$ did not show this form or symmetry. A suggested growth process for similar structures reported in the literature^{13,14} proposes (a) that such faceting can result from preferential lateral growth along the [01-10] [11-00], and [1-010] directions to give the faceted crystallites and (b) that the bevelling can be the interfaces between many independently formed crystallites which combine along the axis of the rod.

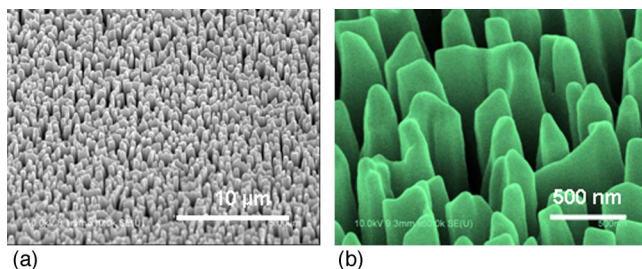


FIG. 6. (Color online) SEM images of ZnO nanostructures grown by PLD on $c\text{-Al}_2\text{O}_3$.

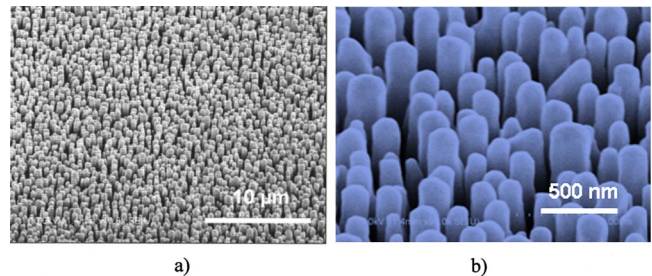


FIG. 7. (Color online) SEM images of ZnO nanostructures grown by PLD on Si (111).

2. SEM images for PVT growth of ZnO

SEM images for PVT growth of ZnO on $c\text{-Al}_2\text{O}_3$. A very wide range of ZnO nanostructures, of varying form and size, were observed for samples grown by PVT on $c\text{-Al}_2\text{O}_3$. No preferred orientation was observed. Figure 4(a) shows pyramidal, faceted structures. Figure 4(b) shows typical nanowire type structures for which a suggested growth mechanism has been proposed elsewhere:^{15,16} the reaction of Zn vapor and O form a hexagonal columnar base on the substrate [Figure 4(a)]. On top of this hexagonal base [the (0001) plane], a nucleation of ZnO particles can occur, leading to a full ZnO hexagonal columnar pin [Fig. 4(b)].

SEM images for PVT growth of ZnO on Si (111). The growth of ZnO on Si (111) by PVT also presented a very wide range of nanostructures of varying form, size, and orientation. Of particular note was a region, expanded in the SEM image in Fig. 5(a), which showed a remarkable ZnO-nanocomb-like structure. A possible growth process for such structures has also been proposed in the literature:¹⁷ at the initial stages of growth, Zn and O combine on the substrate to form a microwire. During subsequent growth, the combined effect of diffusion gradients, different relative growth rates, and thermal perturbations cause inhomogeneous nuclei to form on the surface of the microwire. Nanowires then grow on these nuclei to form the nanocomblike structure. Commonly observed, hexagonally faceted, nanowires were also visible in the same sample [Fig. 5(b)].

3. SEM images for PLD growth of ZnO

SEM images for PLD growth of ZnO on $c\text{-Al}_2\text{O}_3$. Figure 6(a) shows a typical region of sample for the ZnO nanostructures grown on $c\text{-Al}_2\text{O}_3$ by PLD. The image shows a high density array of nanostructures of rather similar shape with a strong preferred orientation perpendicular to the substrate plane. The higher magnification image in Fig. 6(b) reveals that some of these nanostructures look something like incomplete nanotubes. The growth process for such nanostructures is unclear but the structures indicate a preferential growth along both the c -axis and one basal plane axis.¹⁶

SEM images for PLD growth of ZnO on Si (111). In the SEM image shown in Fig. 7(a), an array with a very high density of nanostructures can be seen. The higher magnification image of Fig. 7(b) reveals nanorods of rather uniform shape, typically 200 nm in diameter and 3 μm long. The vast

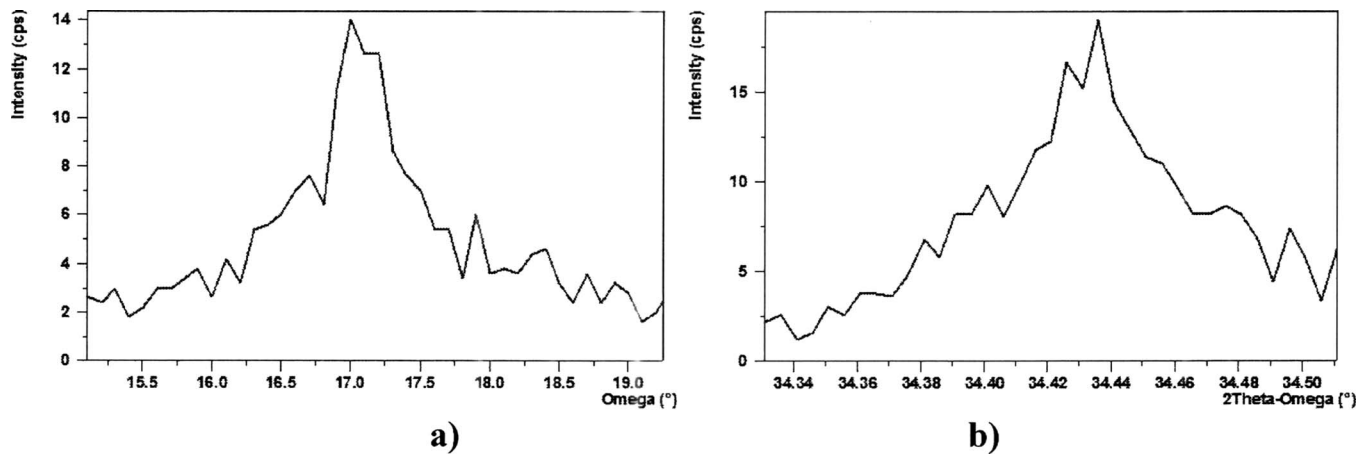


FIG. 8. (a) Omega scans and (b) two theta omega scans for ZnO nanostructures grown by MOCVD on $c\text{-Al}_2\text{O}_3$.

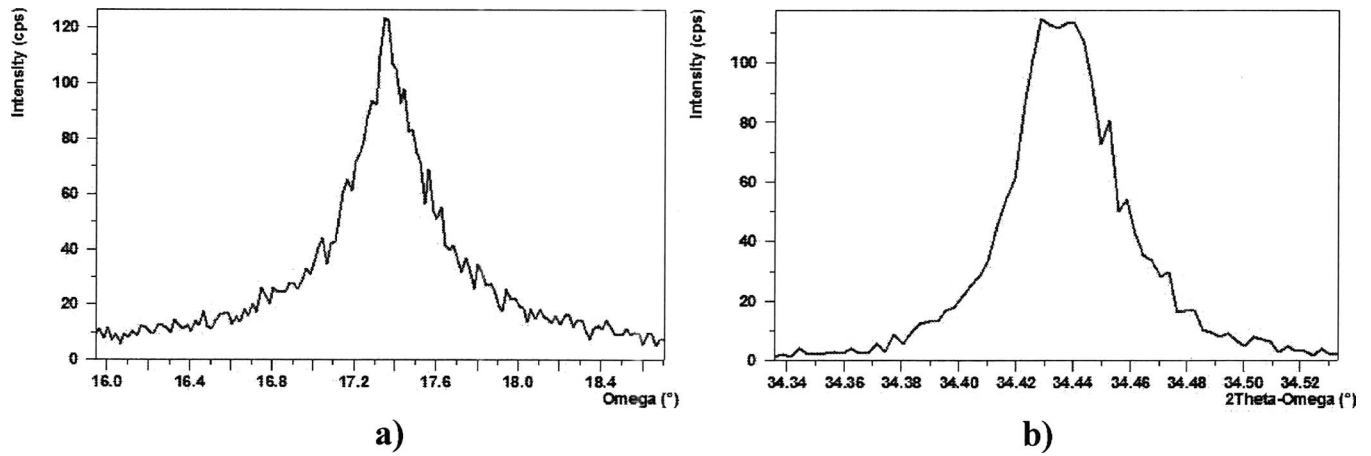


FIG. 9. (a) Omega scans and (b) two theta omega scans for ZnO nanostructures grown by PVT on $c\text{-Al}_2\text{O}_3$.

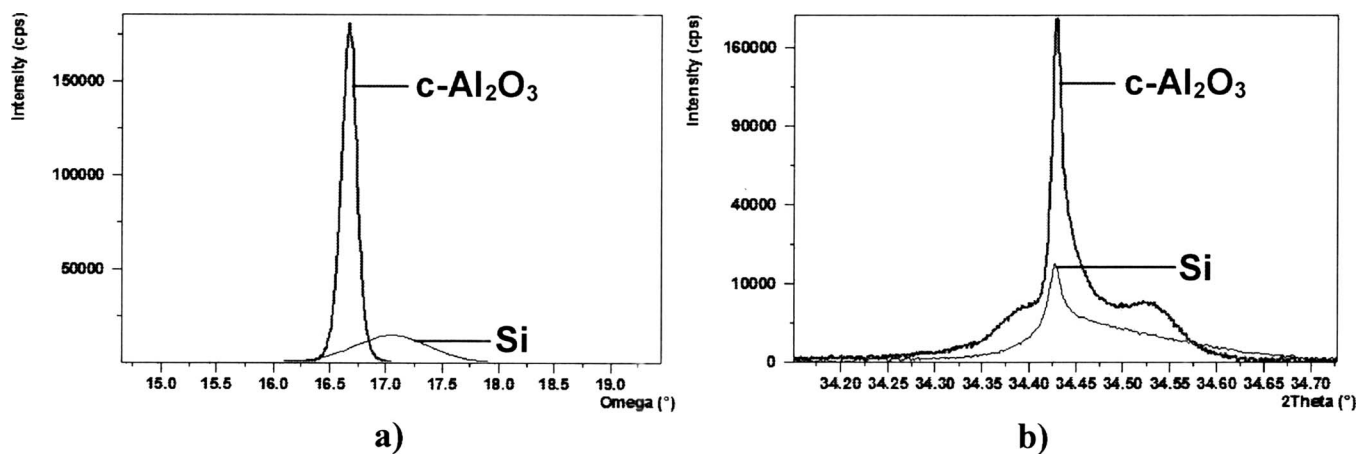


FIG. 10. (a) Omega scans and (b) two theta omega scans for ZnO nanostructures grown by PLD on $c\text{-Al}_2\text{O}_3$ and Si(111).

TABLE I. Comparison of XRD scans intensities and ω -FWHM for ZnO nanostructures grown on *c*-Al₂O₃

Sample	Intensity (counts/s) (cps)	ω rocking curve FWHM (deg)
MOCVD ZnO/ <i>c</i> -Al ₂ O ₃	13	0.56
PVT ZnO/ <i>c</i> -Al ₂ O ₃	107	0.41
PLD ZnO/ <i>c</i> -Al ₂ O ₃	180 974	0.16

majority of the columns is strongly aligned along the perpendicular to the substrate plane. It has been suggested that the shape of such nanostructures could be explained by a preferential hexagonal growth along the *c*-axis plus a secondary preferential growth along the [1011] axis related to different relative crystal growth rates.¹⁶ The relatively homogeneous array of vertically aligned nanorods could be useful for many potential applications such as improved light extraction in LEDs or directional sensitive detectors.

B. XRD investigations

Strong ZnO (0002) reflections corresponding to a *c*-axis oriented wurtzite phase were observed for the samples grown on *c*-Al₂O₃ by all three growth process (Figs. 8–10). The intensity of the XRD peak for the nano-ZnO grown by PLD (Tables I and II) is more than three orders of magnitude higher than those for the structures grown by MOCVD and PVT. Although direct comparison of XRD peak intensity cannot be absolute, SEM study suggested that the volume of ZnO was comparable for all the samples, so the PLD samples appear to be much better crystallized. The ω rocking curve full width at half maximum (FWHM) was smallest for the nanostructures grown by PLD and largest for those grown by MOCVD. For the Si (111) substrate, only the nanostructures grown by PLD gave a response in the XRD analysis (Fig. 10 and Table II). This indicates a relatively poor crystallization on Si (111) compared with that on *c*-Al₂O₃. The *c*-axis lattice constants of the nanostructures were determined from the ZnO (0002) peak position and found to be similar for all the nanostructures (from 5.205 to 5.206 Å) and close to that for relaxed wurtzite ZnO.¹⁸ In summary, the nanostructures grown by PLD appeared to be better crystallized and have less dispersion in crystallographic orientation than the other nanostructures.

TABLE II. Comparison of XRD scans intensities and ω -FWHM for ZnO nanostructures grown on Si(111).

Sample	Intensity (counts/s) (cps)	ω rocking curve FWHM (deg)
MOCVD ZnO/Si (111)	No peak	No peak
PVT ZnO/Si (111)	No peak	No peak
PLD ZnO/Si (111)	15 047	0.79

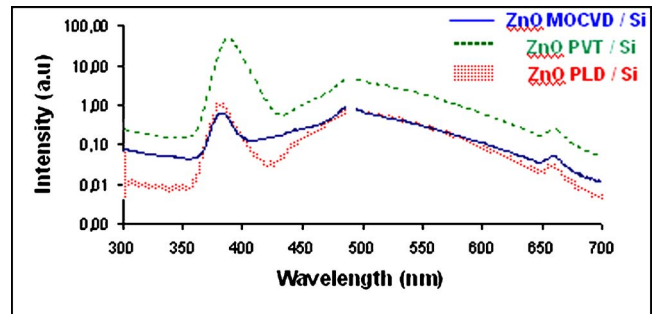


FIG. 11. (Color online) PL spectra for ZnO nanostructures grown on Si(111).

C. PL investigations

PL spectra for all samples (Figs. 11 and 12 and Tables III and IV) showed an ultraviolet (UV) band and a green band [N.B. there is a gap in all spectra at around 488 nm due to the second harmonic peak of the UV laser (244 nm) used for this experiment]. The UV emission was indexed as ZnO near band edge (NBE) emission¹⁹ and the green emission was attributed to defects in the ZnO.²⁰ The NBE emission wavelength and FWHM were lower for the structures grown on Si substrates than for those grown on *c*-Al₂O₃. The NBE emission wavelengths (λ_{max}) were also observed to depend on growth technique. The structures grown by PLD had the shortest NBE λ_{max} (380.0 nm on Si and 380.3 nm on *c*-Al₂O₃) and the structures grown by PVT had the longest λ_{max} (387.5 nm on Si and 391.5 nm on *c*-Al₂O₃). Structures grown by MOCVD had NBE λ_{max} at 382.3 nm on Si and 383.5 nm on *c*-Al₂O₃. The intensity of the PL peak for the nano-ZnO grown on Al₂O₃ and by MOCVD (Table IV) is more than an order of magnitude higher than those for the structures grown by PLD and PVT. The lower NBE λ_{max} and smaller FWHM for structures grown on Si compared to those grown on *c*-Al₂O₃ could be related to Al diffusion from the *c*-Al₂O₃ substrate, which the authors have observed by secondary ion mass spectroscopy in ZnO thin films grown at similar temperatures.²¹

V. CONCLUSION

ZnO nanostructures were grown on Si (111) and *c*-Al₂O₃ substrates by MOCVD, PVT, and PLD. The comparison of nanostructures grown with these three different techniques was complicated by the fact that they gave structures with

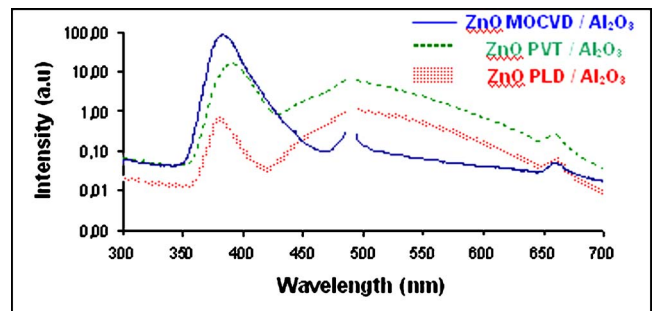
FIG. 12. (Color online) PL spectra for ZnO nanostructures grown on *c*-Al₂O₃.

TABLE III. Comparison of PL spectra, λ (main peak), FWHM, and intensity for ZnO nanostructures grown on Si (111).

Sample	λ (nm)	FWHM (nm)	Intensity (a.u.)
PLD ZnO/Si (111)	380.0	13.0	1.1
MOCVD ZnO/Si (111)	382.3	15.8	0.6
PVT ZnO/Si (111)	387.3	15.3	49.1

different forms and scales. Indeed, SEM revealed a myriad of ZnO nanostructures such as hexagonal nanorods, nanoneedles, and nanotubes along with novel bevelled structures with 12 facets.

PVT growth gave the biggest family of nanostructures. A dense array of regular nanorods with a preferred orientation perpendicular to the substrate plane was obtained on both Si and *c*-Al₂O₃, by PLD, without the use of a catalyst. XRD did not reveal peaks for the structures grown on Si by MOCVD and PVT. XRD scans for the PLD nanostructures grown on *c*-Al₂O₃ gave a much more intense (0002) peak and the smallest ω rocking curve FWHM, suggesting that the PLD structures were very well crystallized and the most highly oriented. PL spectra showed that the nanostructures grown

TABLE IV. Comparison of PL spectra, λ (main peak), FWHM, and intensity for ZnO nanostructures grown on *c*-Al₂O₃.

Sample	λ (nm)	FWHM (nm)	Intensity (a.u.)
PLD ZnO/ <i>c</i> -Al ₂ O ₃	380.3	14.5	0.7
MOCVD ZnO/ <i>c</i> -Al ₂ O ₃	383.5	18.3	81.0
PVT ZnO/ <i>c</i> -Al ₂ O ₃	391.5	22.5	16.2

by PLD had the lowest λ_{\max} and the smallest FWHM. This is consistent with MOCVD having higher impurity doping levels than the PLD. Structures grown on Si had lower λ_{\max} and smaller FWHM than those grown on *c*-Al₂O₃. This redshift and peak broadening on *c*-Al₂O₃ may be related to Al diffusing into the ZnO from the substrate.

¹D. J. Rogers *et al.*, Appl. Phys. Lett. **91**, 071120 (2007).²M. Zerdali, S. Hamzaoui, F. Hosseini Teherani, and D. Rogers, Mater. Lett. **60**, 504 (2006).³V. E. Sandana *et al.*, Proc. SPIE **6895**, 29 (2008).⁴J. Zhong, H. Chen, G. Saraf, Y. Lu, C. K. Choi, and J. J. Song, Appl. Phys. Lett. **90**, 203515 (2007).⁵T. Reuters, Phys. World **21**, 36 (2008).⁶Ü. Özgür, Ya. I. Alivov, C. Liu, A. Teke, M. A. Reshchikov, S. Doğan, V. Avrutin, S.-J. Cho, and H. Morkoç, J. Appl. Phys. **98**, 041301 (2005).⁷H. J. Fan, P. Werner, and M. Zacharias, Biophys. J. **2**, 700 (2006).⁸Z. L. Wang, J. Phys.: Condens. Matter **16**, R829 (2004).⁹Z. Li, R. Yang, M. Yu, F. Bai, C. Li, and Z. L. Wang, J. Phys. Chem. C **112**, 20114 (2008).¹⁰X. Y. Kong and Z. L. Wang, Nano Lett. **3**, 1625 (2003).¹¹D. J. Rogers *et al.*, Phys. Status Solidi C **5**, 3084 (2008).¹²R. Nishimura, T. Sakano, T. Okato, T. Saiki, and M. Obara, Jpn. J. Appl. Phys. **47**, 4799 (2008).¹³V. A. Coleman, J. E. Bradby, C. Jagadish, and M. R. Phillips, Appl. Phys. Lett. **89**, 082102 (2006).¹⁴Z. Li, F. Xu, X. Sun, and W. Zhang, Cryst. Growth Des. **8**, 805 (2008).¹⁵H. Hou, Y. Xiong, Y. Xie, Q. Li, J. Zhang, and X. Tian, J. Solid State Chem. **177**, 176 (2004).¹⁶G. Z. Wang, Y. Wang, M. Y. Yau, C. Y. To, C. J. Deng, and D. H. L. Ng., Mater. Lett. **59**, 3870 (2005).¹⁷X. Tian, F. Pe, J. Fe, C. Yang, H. Luo, D. Luo, and Z. Pi, Physica E **31**, 213 (2006).¹⁸H. Karzel *et al.*, Phys. Rev. B **53**, 11425 (1996).¹⁹Y. C. Kong, D. P. Yu, B. Zhang, W. Fang, and S. Q. Feng, Appl. Phys. Lett. **78**, 407 (2001).²⁰S. A. Studenikim, N. Golego, and M. Cocivera, J. Appl. Phys. **84**, 2287 (1998).²¹D. J. Rogers *et al.*, Proc. SPIE **7217**, 72170F (2009).